

## ANESTHESIOLOGY

# Oral Dimethyl Fumarate Reduces Peripheral Neuropathic Pain in Rodents *via* NFE2L2 Antioxidant Signaling

Jiahe Li, Ph.D., Jiacheng Ma, Ph.D.,  
Michael J. Lacagnina, Ph.D., Sabina Lorca, B.S.,  
Max A. Odem, Ph.D., Edgar T. Walters, Ph.D.,  
Annemieke Kavelaars, Ph.D., Peter M. Grace, Ph.D.

ANESTHESIOLOGY 2020; 132:343–56

## EDITOR'S PERSPECTIVE

### What We Already Know about This Topic

- Oxidative stress is an important driver of neuropathic pain
- Dimethyl fumarate activates nuclear factor erythroid 2-related factor 2, increasing the expression of multiple antioxidant genes

### What This Article Tells Us That Is New

- Using a rat model of nerve injury, both male and female animals displayed reduced mechanical and nociceptive sensitization when given dimethyl fumarate
- Dimethyl fumarate administration increased superoxide dismutase activity while decreasing cytokine expression and improving mitochondrial bioenergetics

Neuropathic pain, caused by nervous system lesion or disease, has an estimated prevalence of 7 to 10% in the general population, and is a tremendous burden to the economy and to the patient's quality of life.<sup>1,2</sup> Pharmacologic treatment of such pain relies primarily upon monoamine reuptake inhibitors, anticonvulsant agents, and opioids.<sup>3</sup> These drugs have only modest efficacy and are also plagued by adverse effects and risk for misuse and abuse.<sup>3,4</sup> Several strategies have been proposed to realize new and nonaddictive treatments for chronic pain, including development of drugs that target endogenous pain resolution mechanisms

## ABSTRACT

**Background:** Available treatments for neuropathic pain have modest efficacy and significant adverse effects, including abuse potential. Because oxidative stress is a key mechanistic node for neuropathic pain, the authors focused on the master regulator of the antioxidant response—nuclear factor erythroid 2-related factor 2 (NFE2L2; Nrf2)—as an alternative target for neuropathic pain. The authors tested whether dimethyl fumarate (U.S. Food and Drug Administration-approved treatment for multiple sclerosis) would activate NFE2L2 and promote antioxidant activity to reverse neuropathic pain behaviors and oxidative stress-dependent mechanisms.

**Methods:** Male Sprague Dawley rats, and male and female wild type and *Nfe2l2*<sup>-/-</sup> mice were treated with oral dimethyl fumarate/vehicle for 5 days (300 mg/kg; daily) after spared nerve injury/sham surgery (n = 5 to 8 per group). Allodynia was measured in von Frey reflex tests and hyperalgesia in operant conflict-avoidance tests. Ipsilateral L4/5 dorsal root ganglia were assayed for antioxidant and cytokine/chemokine levels, and mitochondrial bioenergetic capacity.

**Results:** Dimethyl fumarate treatment reversed mechanical allodynia (injury-vehicle, 0.45 ± 0.06 g [mean ± SD]; injury-dimethyl fumarate, 8.2 ± 0.16 g; *P* < 0.001) and hyperalgesia induced by nerve injury (injury-vehicle, 2 of 6 crossed noxious probes; injury-dimethyl fumarate, 6 of 6 crossed; *P* = 0.013). The antiallodynic effect of dimethyl fumarate was lost in nerve-injured *Nfe2l2*<sup>-/-</sup> mice, but retained in nerve-injured male and female wild type mice (wild type, 0.94 ± 0.25 g; *Nfe2l2*<sup>-/-</sup>, 0.02 ± 0.01 g; *P* < 0.001). Superoxide dismutase activity was increased by dimethyl fumarate after nerve injury (injury-vehicle, 3.96 ± 1.28 mU/mg; injury-dimethyl fumarate, 7.97 ± 0.47 mU/mg; *P* < 0.001). Treatment reduced the injury-dependent increases in cytokines and chemokines, including interleukin-1β (injury-vehicle, 13.30 ± 2.95 pg/mg; injury-dimethyl fumarate, 6.33 ± 1.97 pg/mg; *P* = 0.022). Injury-impaired mitochondrial bioenergetics, including basal respiratory capacity, were restored by dimethyl fumarate treatment (*P* = 0.025).

**Conclusions:** Dimethyl fumarate, a nonopioid and orally-bioavailable drug, alleviated nociceptive hypersensitivity induced by peripheral nerve injury *via* activation of NFE2L2 antioxidant signaling. Dimethyl fumarate also resolved neuroinflammation and mitochondrial dysfunction—oxidative stress-dependent mechanisms that drive nociceptive hypersensitivity after nerve injury.

(ANESTHESIOLOGY 2020; 132:343–56)

and that simultaneously modify multiple pathophysiological mechanisms that underlie pain.<sup>5,6</sup>

Drugs that target oxidative stress may meet these challenges. In rodent models of peripheral neuropathic pain, reactive oxygen species are elevated in dorsal root ganglia neurons and in glia and immune cells.<sup>7–9</sup> Reactive oxygen species promote hyperexcitability of dorsal root ganglia

Supplemental Digital Content is available for this article. Direct URL citations appear in the printed text and are available in both the HTML and PDF versions of this article. Links to the digital files are provided in the HTML text of this article on the Journal's Web site ([www.anesthesiology.org](http://www.anesthesiology.org)).

Submitted for publication April 24, 2019. Accepted for publication October 3, 2019. Published online first on December 9, 2019. From the Laboratories of Neuroimmunology, Department of Symptom Research, The University of Texas MD Anderson Cancer Center (J.L., J.M., M.J.L., S.L., A.K., P.M.G.); and the Department of Integrative Biology and Pharmacology, McGovern Medical School at UTHealth (M.A.O., E.T.W.), Houston, Texas.

Copyright © 2020, the American Society of Anesthesiologists, Inc. All Rights Reserved. Anesthesiology 2020; 132:343–56. DOI: 10.1097/ALN.0000000000003077

neurons *via* several mechanisms, including disrupted mitochondrial bioenergetics, which impairs energy production and ion homeostasis and leads to spontaneous activity and degeneration of nociceptors.<sup>7</sup> These reactive species also indirectly induce neuronal hyperexcitability by promoting expression of neuroinflammatory mediators (*e.g.*, activation of nuclear factor  $\kappa$ -light-chain-enhancer of activated B cells).<sup>7,8,10,11</sup> Therefore, restoring redox balance has the potential to resolve multiple pain mechanisms.

There have been many attempts to pharmacologically control oxidative stress in chronic pain states; to date, none are in clinical use. Supplementation of individual antioxidants has not only failed due to unfavorable pharmacokinetics and pharmacodynamics, but also because numerous antioxidants are required to restore homeostasis by collaboratively catabolizing reactive oxygen species.<sup>7,8</sup> For this reason, we have focused on the transcription factor nuclear factor erythroid 2-related factor 2 (NFE2L2; Nrf2). Under physiologic conditions, NFE2L2 is sequestered in the cytosol by Kelch-like ECH associated-protein 1 (Keap1) and ubiquitinated for degradation. However, oxidants and electrophiles trigger release of NFE2L2 from Keap1, translocation to the nucleus, and binding to the antioxidant response element that initiates transcription of more than 200 antioxidant-related genes.<sup>12,13</sup> Thus, NFE2L2 is an attractive therapeutic target to stimulate endogenous production of the multiple antioxidants required to simultaneously detoxify a range of reactive oxygen species.

Investigation of the disease-modifying potential of NFE2L2 activation for neuropathic pain is limited. NFE2L2 activators sulforaphane and cobalt protoporphyrin are antinociceptive in several rodent models of neuropathic pain.<sup>14–19</sup> To date, these agents have not been clinically translated, and there has been little investigation of the therapeutic effects on known pain mechanisms. Here, we evaluated the therapeutic actions of dimethyl fumarate in the rat spared nerve injury model of peripheral neuropathic pain. Dimethyl fumarate—approved by the U.S. Food and Drug Administration and the European Medicines Agency for treatment of relapsing–remitting multiple sclerosis<sup>20,21</sup>—activates NFE2L2 by disrupting the NFE2L2–Keap1 complex.<sup>22,23</sup> We hypothesized that dimethyl fumarate would reverse spared nerve injury–induced nociceptive hypersensitivity and attendant mitochondrial dysfunction and neuroinflammation in an NFE2L2-dependent manner. The primary outcome was mechanical allodynia, while the secondary outcomes were mechanical hyperalgesia and biochemical measures.

## Materials and Methods

### Animals

Pathogen-free adult male Sprague Dawley rats (10 weeks old on arrival; Envigo, USA) were used. Rats were housed two to three per cage in a light- and temperature-controlled room (12:12-h light–dark cycle, lights on at 7:00 AM) with food and water available *ad libitum*. Pretreatment weights

ranged from 309 to 342 g. Male and female (10 to 14 weeks old) wild type and *Nfe2l2*<sup>−/−</sup> mice on a C57BL/6J genetic background (Jackson Laboratory, USA) were housed (five per cage) and bred at The University of Texas MD Anderson Cancer Center (Houston, Texas). The animal facility is pathogen-free and accredited by the Association for Assessment and Accreditation of Laboratory Animal Care. Pretreatment weights ranged from 19 to 26 g. To detect a reversal of von Frey threshold from 0.4 to 4 g with a SD of 0.41 g, a two-tailed power calculation indicated that  $n = 5$  rats per group would be sufficient with Type I error set at 0.05 and the power at 90%. The expected variance for biochemical outcomes is smaller, and therefore a group size of 5 rats would be sufficient for these measures as well. The rats were randomly assigned to groups using a random number generator (GraphPad, USA). No animals were excluded from this study for any reason. All procedures were approved by the MD Anderson Cancer Center Institutional Animal Care and Use Committee and conformed to the National Academy of Science Guide for the Care and Use of Laboratory Animals.

### Spared Nerve Injury Surgery

Spared nerve injury surgery was performed as described for rats<sup>24</sup> and mice,<sup>25</sup> leaving the sural nerve intact, under inhaled isoflurane anesthesia (2 to 4% volume in  $1\text{ l} \cdot \text{min}^{-1}$  oxygen). The surgical plane of anesthesia was verified by areflexia. Ophthalmic ointment was applied to the eyes before surgery commenced. Identical procedures were used for sham surgery, but the nerves were not ligated or transected. Naïve rats were left undisturbed in their home cages. Animals were monitored postoperatively until fully ambulatory before return to their home cage. All surgeries took place between 9:00 AM and 2:00 PM. Postoperative analgesia was not provided so as not to confound the endpoints under study.

### Drug Administrations

Dimethyl fumarate (Sigma-Aldrich, USA) was suspended in methylcellulose (viscosity 15 cP, 2% w · v<sup>−1</sup> in water; ACROS, Belgium) and administered by oral gavage. In our preliminary experiment, rats received escalating daily doses of dimethyl fumarate (days 1 and 2, 30 mg · 5 ml<sup>−1</sup> · kg<sup>−1</sup>; days 3 and 4, 100 mg · 5 ml<sup>−1</sup> · kg<sup>−1</sup>; days 5 to 7, 300 mg · 5 ml<sup>−1</sup> · kg<sup>−1</sup>) beginning 14 days after spared nerve injury/sham surgery. In all subsequent experiments, rats and mice were administered dimethyl fumarate for 5 days (300 mg · 5 ml<sup>−1</sup> · kg<sup>−1</sup>; once per day), beginning 14 days after spared nerve injury/sham surgery. Dosing took place from 8:00 to 10:00 AM. Trigonelline (Cayman Chemical, USA) was suspended in methylcellulose and administered to rats by oral gavage for 5 days (300 mg · 5 ml<sup>−1</sup> · kg<sup>−1</sup>; twice per day), beginning 14 days after spared nerve injury/sham surgery. Dosing took place from 8:00 to 10:00 AM and 4:00 to 6:00 PM. Equivolume methylcellulose (2% w · v<sup>−1</sup>) was used as vehicle control for both drugs. An independent investigator dosed the rats in order to maintain

blinding to treatment groups for the other investigators who performed the behavioral testing and assays.

### Mechanical Allodynia

Testing was conducted blind with respect to group assignment. Rats received at least three 60-min habituations to the test environment before behavioral testing. Rodents were placed in a small plexiglass enclosure on a mesh stand. The von Frey test<sup>26</sup> was performed as described previously for rats<sup>27,28</sup> and mice,<sup>29</sup> between 2 and 4 h of dosing and finishing before 12:00 PM. The behavioral responses were used to calculate absolute threshold (the 50% probability of response) by fitting a Gaussian integral psychometric function using a maximum-likelihood fitting method.<sup>30,31</sup>

### Mechanical Conflict-avoidance

Voluntary aversion to a noxious stimulus was assessed using a commercial three-chambered apparatus, the Mechanical Conflict-Avoidance System (Noldus, USA). The apparatus presents rats with a choice in responding to two aversive stimuli—either to remain exposed to an aversive bright light in one chamber or to escape the light by crossing a middle chamber having a floor covered by a dense array of sharp probes, in order to reach a dark, safe chamber. Longer latencies to escape the light chamber indicate increased motivation to avoid the probes, and this escape latency is currently the most common measure of pain-related behavior in this test. We performed the operant mechanical conflict-avoidance test<sup>32</sup> on rats with modifications as recently described in detail.<sup>33</sup> Naïve rats were used in the control group, as we have previously shown that this assay is highly sensitive to postoperative pain after sham surgery.<sup>33</sup> The test was performed during 2 days, with each day consisting of three 300-s trials. Testing was performed between 8:00 AM and 2:00 PM. In each trial: (1) a rat was placed inside the light chamber with the lid closed, the light off, and the exit door closed; (2) after 20 s the light was turned on; (3) after 15 s the exit door was opened when (or if) the rat faced the exit; (4) the rat freely explored all three chambers in the apparatus for 300 s; (5) the rat was returned to its home cage; and (6) the device was thoroughly cleaned with 70% ethanol and distilled water in preparation for the next trial. On day 1 (the third day of drug treatment), the probe height was set to 0 mm for all three trials. On day 2 (the fourth day of drug treatment), the probe height was set to 0 mm for the first trial, and then raised to 4 mm for the second and third trials. Data are presented as the latency to enter the dark compartment during the third trial on day 2.

### Tissue Collection

Within 4 h of the final dose on day 5, rats were deeply anesthetized with Beuthanasia-D (approximately 100 mg/kg pentobarbital, 13 mg/kg phenytoin [intraperitoneal]; Merck, USA) and then perfused with ice-cold saline. The

ipsilateral lumbar dorsal root ganglia (L4/5) were then isolated. For immunohistochemistry, the saline perfusion was followed by ice-cold 4% paraformaldehyde in 0.1 M phosphate buffer (pH 7.4).

### Immunohistochemistry

L4/5 dorsal root ganglia were postfixed in 4% paraformaldehyde overnight at 4°C. Tissues were cryoprotected stepwise in 15%, 22%, and 30% sucrose in 0.1 M phosphate buffer, supplemented with 0.01% sodium azide (Sigma-Aldrich). After freeze-mounting in optimal cutting temperature compound (Sakura Finetek, USA), tissues were serially sectioned at 10 µm across 10 slides. Each slide contained five sections per dorsal root ganglia so that 10 sections, per animal, were analyzed. Sections were incubated with blocking buffer (2% bovine serum albumin [Sigma-Aldrich], 5% normal goat serum [Abcam, USA], and 0.1% saponin [Sigma-Aldrich] in phosphate buffered saline) overnight at 4°C. Primary antibodies were added after washing and incubated at 4°C for 21 h. Subsequently, sections were washed, then incubated with secondary antibodies for 2 h at room temperature. Primary antibodies used were anti-NFE2L2 antibody (1:500; rabbit polyclonal IgG; Abcam) and anti-activating transcription factor 3 (ATF3) antibody (1:500; mouse monoclonal IgG1; Santa Cruz Biotechnology, USA). Secondary antibodies used were goat antirabbit antibody and donkey antimouse antibody (1:500; ThermoFisher Scientific, USA). Fluorescent photomicrographs were captured using an SPE Leica Confocal Microscope (Leica Microsystems, USA) and an Olympus BX53 microscope with a mercury lamp (U-HGLGPS; Olympus Corporation, Japan). Sections were analyzed using LAS X software (Leica) and cellSens imaging software (Olympus).

### Western Blotting

Nuclear fractions from ipsilateral L4/5 dorsal root ganglia of each rat were isolated with a NE-PER Nuclear and Cytoplasmic Extraction Kit (ThermoFisher Scientific), according to manufacturer instructions. Western blotting was performed as previously described.<sup>28,34,35</sup> In brief, extracted nuclear proteins were subjected to NuPAGE Bis-Tris (4 to 12%) gel electrophoresis under reducing conditions (ThermoFisher Scientific) and then electrophoretically transferred to nitrocellulose membranes (Bio-Rad, USA). Nonspecific binding sites on the membrane were blocked with Superblock buffer containing 0.1% Tween-20, 0.05% Tris-Chloride, and 0.03% 5 M NaCl for 1 h at 22° to 24°C. Membranes were subsequently incubated overnight at 4°C with primary anti-NFE2L2 antibody (1:1,000; rabbit polyclonal IgG; Abcam) and antihistone H3 antibody (1:2,000; rabbit polyclonal IgG; Abcam) (loading control) in blocking buffer containing 0.1% Tween-20. The membranes were then washed with phosphate buffered saline

containing 0.1% Tween-20, and probed with horseradish peroxidase secondary antibody (1:5,000; goat polyclonal IgG; Jackson ImmunoResearch, USA) in blocking buffer containing 0.1% Tween-20 for 1 h at 22° to 24°C. After washing with phosphate buffered saline containing 0.1% Tween-20, membranes were developed with enhanced chemiluminescent substrate (ThermoFisher Scientific), and scanned on an ImageQuant LAS 4,000 mini (GE, USA). Densitometry analysis was performed using ImageQuant TL software (GE). Data were normalized to loading control (histone H3).

### Real-time Polymerase Chain Reaction

Total RNAs were extracted using TRIzol (ThermoFisher Scientific) from the dorsal root ganglia tissues. One  $\mu$ g RNA was used for reverse transcription with iScript Reverse Transcription Supermix (Bio-Rad). Real-time polymerase chain reaction was carried out in a final volume of 20  $\mu$ l with iTaq Universal SYBR Green Supermix (Bio-Rad) containing 2  $\mu$ l of five times diluted cDNA and monitored by CFX Connect Real-Time PCR Detection System (Bio-Rad). The following cycling parameters were used: 95°C for 3 min, 40 cycles of 95°C for 5 s, and 60°C for 30 s. Primer sequences are reported in Supplemental Digital Content 1 (<http://links.lww.com/ALN/C136>). The level of the target mRNA was quantified relative to the house-keeping gene (*Gapdh*) using the  $\Delta\Delta C_T$  method. *Gapdh* was not significantly different between treatments.

### Assay Kits

Dorsal root ganglia were dissociated with a mortar and pestle in tissue extraction reagent supplied with protease and phosphatase inhibitors as previously described.<sup>27,28</sup> Assay kits for glutathione (703002; Cayman Chemical, USA) (detection range, 0.25 to 16  $\mu$ M) superoxide dismutase (706002; Cayman Chemical) (detection range, 0.005 to 0.050 U/ml), DNA/RNA oxidative damage (589320; Cayman Chemical) (detection range, 10.3 to 3,000 pg/ml), interleukin-1  $\beta$  (IL-1 $\beta$ ) (RLB00; R&D Systems, USA) (detection range, 5 to 2,000 pg/ml), tumor necrosis factor (TNF) (RTA00; R&D Systems) (detection range: 5 to 800 pg/ml), and C-C motif chemokine ligand 2 (CCL2) (ab100778; Abcam) (detection range, 24.67 to 18,000  $\mu$ M), were used according to manufacturer instructions. Results were normalized to total protein levels (Bradford protein assay).

### Mitochondrial Bioenergetics

Analysis of mitochondrial bioenergetics was performed in dissociated dorsal root ganglia neurons using the Seahorse assay as previously described.<sup>29,36</sup> Oxygen consumption rate, including basal respiration, adenosine triphosphate-linked respiration, proton leak, and maximal respiratory capacity, were determined as described previously by subtracting nonmitochondrial respiration.<sup>29</sup> Total protein levels

quantified using standard Bradford protein assay in each well were used to normalize each oxygen consumption rate value.

### Statistics

The Shapiro–Wilk test was performed to increase confidence that the data were normally distributed, while the Grubbs' test indicated that there were no outliers in our dataset. Mechanical allodynia was analyzed as the interpolated 50% thresholds (absolute threshold). Where appropriate, one-way ANOVAs or unpaired *t* tests were used to confirm that there were no baseline differences in absolute thresholds between treatment groups. Differences between treatment groups were determined using repeated measures two-way or three-way ANOVA, followed by Tukey *post hoc* tests, where appropriate. For the mechanical conflict avoidance assay, the rats were divided into two groups: those that entered the dark compartment at any time during the 300-s trial and those that did not. Data were analyzed using chi-square tests. For biochemical assays, data were analyzed either by unpaired *t* tests or by two-way ANOVA followed by Tukey *post hoc* tests, as appropriate. Analyses were performed using Prism 8 (GraphPad). Complete statistical methods, comparisons, and results (F-statistics, *P* values, and 95% CI) are presented in Supplemental Digital Content 2 (<http://links.lww.com/ALN/C137>). There were no missing data. Results are expressed as mean  $\pm$  SD. *P* < 0.05 was considered statistically significant.

## Results

### Effects of Dimethyl Fumarate on Reflex and Operant Nociceptive Measures

We assessed the antinociceptive effect of oral dimethyl fumarate treatment on established pain-related behaviors induced by spared nerve injury. In a preliminary experiment, cumulative dose escalation of dimethyl fumarate was evaluated to identify an effective dose. Dimethyl fumarate attenuated spared nerve injury-induced allodynia (time  $\times$  treatment:  $F_{6,36} = 2.79$ ; *P* = 0.025; time,  $F_{3,36} = 2.45$ ; *P* = 0.079; treatment,  $F_{2,36} = 166.9$ ; *P* < 0.001). *Post hoc* analyses revealed that this drug was effective at 300 mg/kg, (*P* = 0.007), but not at lower doses (fig. 1A). To confirm the therapeutic efficacy of this dose in an independent experiment, dimethyl fumarate was administered daily for 5 days, beginning 14 days after spared nerve injury or sham surgery. Within 3 days, dimethyl fumarate treatment completely reversed mechanical allodynia ( $8.2 \pm 0.16$  g), compared to vehicle treatment ( $0.45 \pm 0.06$  g), an effect that was maintained until dosing conclusion (fig. 1B; time  $\times$  injury  $\times$  treatment,  $F_{4,80} = 17.4$ ; *P* < 0.001; injury  $\times$  treatment,  $F_{1,20} = 96.6$ ; *P* < 0.001; time  $\times$  treatment,  $F_{4,80} = 28.0$ ; *P* < 0.001; time  $\times$  injury,  $F_{4,80} = 21.6$ ; *P* < 0.001; treatment,  $F_{1,20} = 138$ ; *P* < 0.001; injury,  $F_{1,20} = 467$ ; *P* < 0.001; time,  $F_{4,80} = 23.5$ ; *P* < 0.001). In this



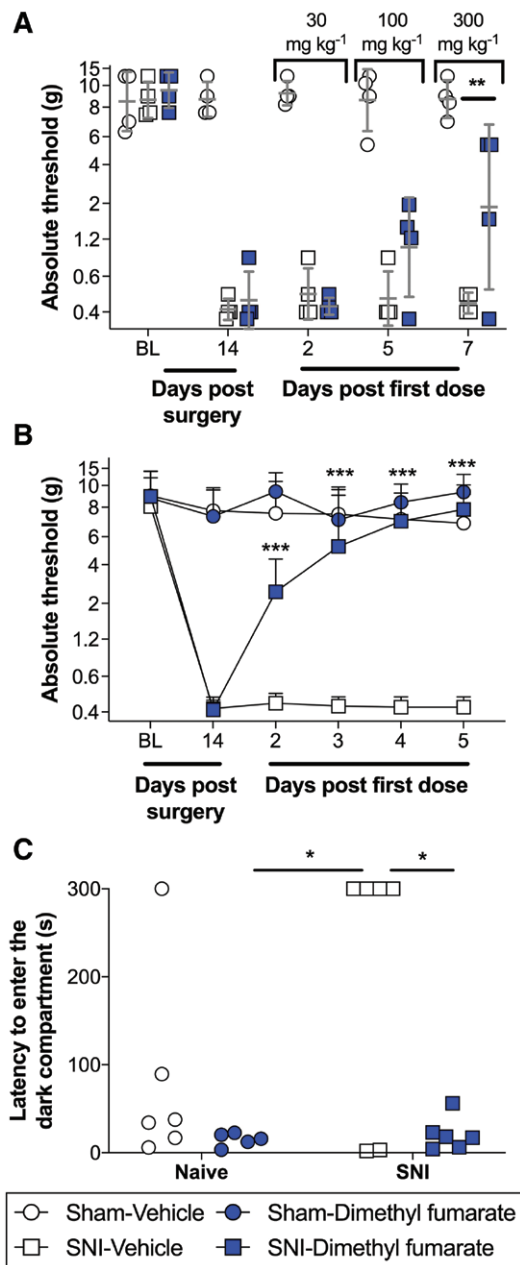


**Fig. 1.** Effects of dimethyl fumarate treatment on reflexive and operant nociceptive measures after spared nerve injury (SNI). (A) Beginning 14 days after SNI or sham surgery, dimethyl fumarate or vehicle was orally administered once per day for 7 days (days 1 and 2, 30 mg/kg; days 3 and 4, 100 mg/kg; days 5 to 7, 300 mg/kg). Mechanical allodynia was assessed using the von Frey test. SNI-induced allodynia was attenuated by dimethyl fumarate in a dose-dependent fashion.  $n = 4$  rats/group. (B, C) Beginning 14 days after SNI or sham surgery, dimethyl fumarate or vehicle was orally administered for 5 days (300 mg/kg; once per day). (B) Von Frey thresholds for mechanical allodynia.  $n = 6$  rats/group. (C) Latency to cross noxious probes and enter the dark compartment during the final 300-s mechanical conflict-avoidance test after 4 days of treatment.  $n = 5$  in the naive-dimethyl fumarate group,  $n = 6$  rats in all other groups. Data are mean  $\pm$  SD or individual data points; \* $P < 0.05$ , \*\* $P < 0.01$ , \*\*\* $P < 0.001$ .

experiment, we also noted a reduction in body weight in the dimethyl fumarate treated group ( $274 \pm 13$  g), compared to the vehicle treated group ( $325 \pm 9$  g;  $P < 0.001$ ).

The operant mechanical conflict-avoidance test was used to further evaluate the antinociceptive properties of dimethyl fumarate in a task where mechanical stimulation is voluntary. Only two of six rats from the spared nerve injury-vehicle group crossed the 4-mm probes and entered the dark compartment. In contrast, six of six rats from the spared nerve injury-dimethyl fumarate group entered the dark compartment; this increased proportion of rats that crossed the noxious probes was statistically significant compared to the spared nerve injury-vehicle group ( $P = 0.013$ ) (fig. 1C). At 0 mm (*i.e.*, probes absent), all rats entered the dark compartment within 15 s (data not shown).

### NFE2L2 Activation by Dimethyl Fumarate in Dorsal Root Ganglia

To determine whether dimethyl fumarate could activate NFE2L2 in the dorsal root ganglia as predicted (that is, induce nuclear translocation), we next examined NFE2L2 colocalization with the nuclear stain 4',6-diamidino-2-phenylindole using immunohistochemistry (injury  $\times$  treatment,  $F_{1,22} = 7.01$ ;  $P = 0.015$ ; injury,  $F_{1,22} = 0.428$ ;  $P = 0.520$ ; treatment,  $F_{1,22} = 72.07$ ;  $P < 0.001$ ). Dimethyl fumarate treatment increased the proportion of NFE2L2<sup>+</sup> nuclei in both the sham (51 NFE2L2<sup>+</sup> nuclei of 81 total nuclei  $\pm$  22 of 29;  $P < 0.001$ ) and spared nerve injury groups (60 of 125  $\pm$  17 of 52;  $P = 0.002$ ), compared to the sham-vehicle group (18 of 114  $\pm$  10 of 34) (fig. 2A). We found that the proportion of NFE2L2<sup>+</sup> nuclei increased in the sample nerve injury-vehicle group (22 of 102  $\pm$  8 of 34) compared to sham-vehicle was not statistically significant ( $P = 0.538$ ). Representative photomicrographs are presented in figure 2B.

We also measured NFE2L2 protein levels in the nuclear extracts using Western blotting as an orthogonal approach (fig. 2, C and D; injury  $\times$  treatment,  $F_{1,16} = 0.35$ ;  $P = 0.561$ ; injury,  $F_{1,16} = 0.01$ ;  $P = 0.966$ ; treatment,  $F_{1,16} = 33.0$ ;  $P < 0.001$ ). *Post hoc* tests showed that dimethyl fumarate treatment increased levels of NFE2L2 in the sham group ( $P = 0.002$ ) and spared nerve injury group ( $P = 0.011$ ). NFE2L2 levels were not increased in the spared nerve injury-vehicle group, compared to sham-vehicle ( $P = 0.969$ ). Representative blots are presented in figure 2D.

### Effects of Dimethyl Fumarate on Antioxidant Expression and Activity

Because NFE2L2 activation drives expression of antioxidants, we evaluated the effect of dimethyl fumarate treatment on both the expression and activity of two representative antioxidants in dorsal root ganglia after spared nerve injury: glutathione and superoxide dismutase. These antioxidants are responsible for catabolism of superoxide,

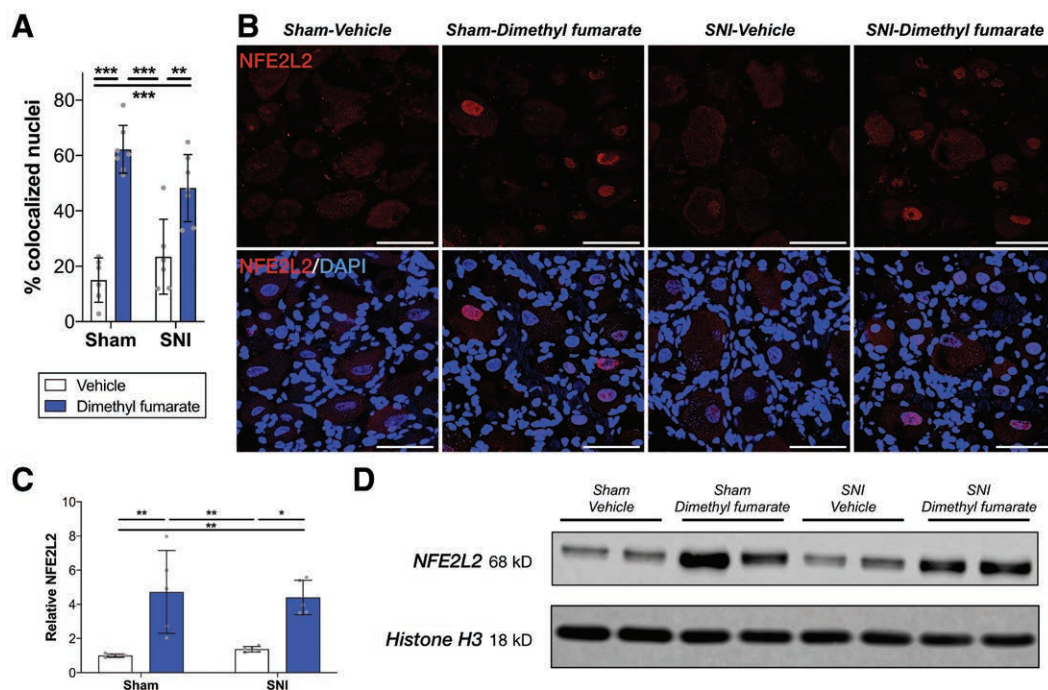


**Fig. 2.** Nuclear factor erythroid 2-related factor 2 (NFE2L2) activation in lumbar dorsal root ganglia (DRG). (A to D) Ipsilateral L4/5 DRG were collected after 5 days of oral dimethyl fumarate treatment (300 mg/kg; once per day) or vehicle, which began 14 days after spared nerve injury (SNI)/sham surgery. (A) NFE2L2 and nuclei were immunofluorescently labeled in DRG sections. The number of DAPI-positive nuclei colocalized with NFE2L2 are expressed as a percentage of the total number of nuclei in each section. (B) Representative fluorescent photomicrographs are presented (40 $\times$ ). Scale bar = 50  $\mu$ m. (C) NFE2L2 protein levels were assayed in nuclear extracts using Western blotting. Blot density (normalized to histone H3 loading control) and relative to the sham-vehicle condition is presented. (D) Representative blots are presented. Data are mean  $\pm$  SD; \* $P$  < 0.05, \*\* $P$  < 0.01, \*\*\* $P$  < 0.001; DRG from  $n$  = 6 rat/group.

hydrogen peroxide and hydroxyl radicals.<sup>7</sup> The expression of several genes involved in glutathione synthesis and activity were quantified. Dimethyl fumarate treatment increased expression of *Gclm* (fig. 3A; injury  $\times$  treatment,  $F_{1,20}$  = 4.78;  $P$  = 0.041; injury,  $F_{1,20}$  = 3.83;  $P$  = 0.065; treatment,  $F_{1,20}$  = 11.13;  $P$  = 0.003) and *Gclc* (fig. 3B; injury  $\times$  treatment,  $F_{1,20}$  = 0.26;  $P$  = 0.616; injury,  $F_{1,20}$  = 1.65;  $P$  = 0.214; treatment,  $F_{1,20}$  = 14.0,  $P$  = 0.001), which encode subunits of glutamate-cysteine ligase (the first rate limiting enzyme in glutathione synthesis). The gene encoding glutathione reductase, *Gsr*, which catalyzes the reduction of glutathione disulfide to glutathione sulfhydryl, was not altered by dimethyl fumarate treatment (fig. 3C; injury  $\times$  treatment,  $F_{1,20}$  = 0.95;  $P$  = 0.341; injury,  $F_{1,20}$  = 0.17;  $P$  = 0.687; treatment,  $F_{1,20}$  = 1.94;  $P$  = 0.179). *Gclm*, but not *Gclc* or *Gsr*, was decreased in the spared nerve injury-vehicle group compared to sham-vehicle ( $P$  = 0.038) (fig. 3, A to C). Dimethyl fumarate treatment increased total glutathione protein levels in the dorsal root ganglia ( $4.23 \pm 0.49$  nmol/mg protein) compared to spared nerve injury-vehicle ( $2.81 \pm 0.37$  nmol/mg protein) (fig. 3D; injury  $\times$  treatment:  $F_{1,20}$  = 7.11;  $P$  = 0.015; injury,  $F_{1,20}$  = 1.91;  $P$  = 0.183; treatment,  $F_{1,20}$  = 15.44;  $P$  < 0.001). Furthermore, total glutathione

protein levels were decreased by spared nerve injury compared to sham-vehicle ( $3.68 \pm 0.68$  nmol/mg protein;  $P$  = 0.044) (fig. 3D). There was no effect of dimethyl fumarate in the sham groups.

Dimethyl fumarate treatment rescued expression of *Sod1* (fig. 3E; injury  $\times$  treatment,  $F_{1,20}$  = 2.80;  $P$  = 0.110; injury,  $F_{1,20}$  = 8.00;  $P$  = 0.010; treatment,  $F_{1,20}$  = 13.82;  $P$  < 0.001) and *Sod2* (fig. 3F; injury  $\times$  treatment,  $F_{1,20}$  = 10.5;  $P$  = 0.004; injury,  $F_{1,20}$  = 3.23;  $P$  = 0.087; treatment,  $F_{1,20}$  = 27.3;  $P$  < 0.001), which respectively encode the superoxide dismutase isoforms found in the cytosol and mitochondria (fig. 3, E and F). Compared to sham-vehicle, *Sod1* ( $P$  = 0.022) and *Sod2* ( $P$  = 0.010) levels were both downregulated by spared nerve injury (fig. 3, E and F). Activity levels of total superoxide dismutase were also restored by dimethyl fumarate treatment (injury-vehicle,  $3.96 \pm 1.28$  mU/mg; injury-dimethyl fumarate,  $7.97 \pm 0.47$  mU/mg), though enzyme activity was not attenuated by spared nerve injury compared to sham-vehicle ( $5.46 \pm 1.50$  mU/mg) (fig. 3G; injury  $\times$  treatment,  $F_{1,20}$  = 15.19;  $P$  < 0.001; injury,  $F_{1,20}$  = 0.33;  $P$  = 0.573; treatment,  $F_{1,20}$  = 24.72;  $P$  < 0.001). Once again, there was no effect of dimethyl fumarate in the sham groups.

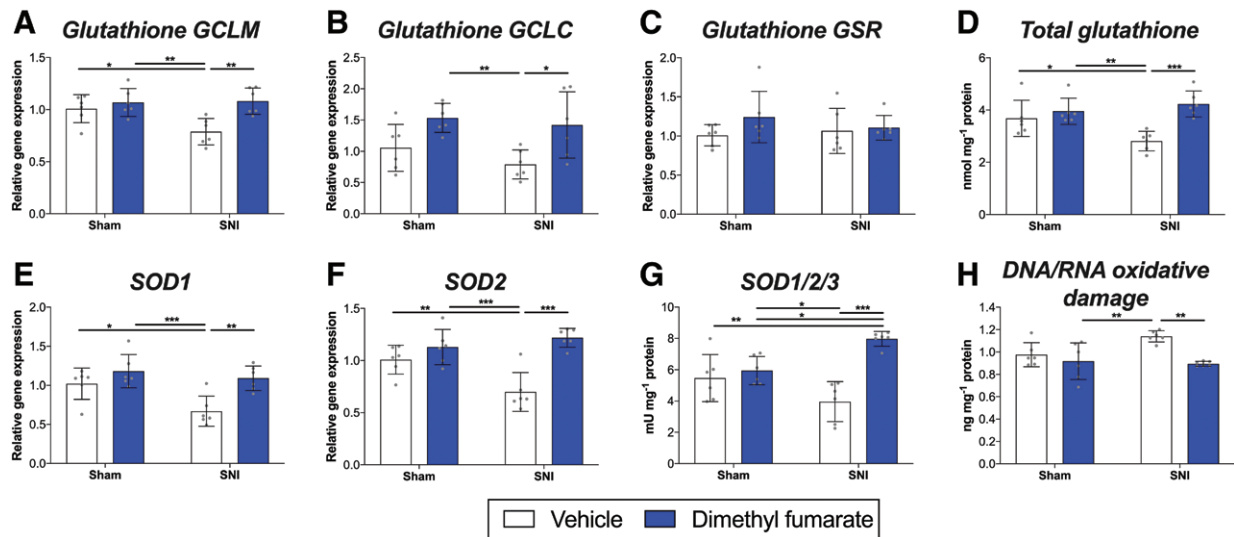


**Fig. 3.** Effects of dimethyl fumarate treatment on antioxidants and oxidized DNA/RNA after spared nerve injury (SNI). Ipsilateral L4/5 dorsal root ganglia (DRG) were collected after 5 days of oral dimethyl fumarate (DMF) treatment (300 mg/kg; once per day) or vehicle (Veh), which began 14 days after SNI/sham surgery. Messenger RNA (mRNA) expression was quantified for enzymes involved in glutathione synthesis and activity (A) *Gclm*, (B) *Gclc*, (C) *Gsr*, (D) as well as total glutathione protein levels. mRNA for superoxide dismutase (SOD) isoforms (E) *Sod1*, (F) *Sod2*, and (G) total SOD activity were quantified. (H) Levels of 8-oxo-2-deoxyguanosine (8-oxo-dG)/ 8-oxoguanine (8-oxo-G), a marker of DNA/RNA oxidative damage. Data are mean  $\pm$  SD; \* $P < 0.05$ , \*\* $P < 0.01$ , \*\*\* $P < 0.001$ ; DRG from  $n = 6$  rats/group.

Finally, to test whether dimethyl fumarate treatment could attenuate oxidative stress, we examined oxidized DNA/RNA. 8-oxoguanine and 8-oxo-2-deoxyguanosine are common nucleic acid lesions induced by reactive oxygen species. Dimethyl fumarate treatment reduced DNA/RNA oxidation ( $0.89 \pm 0.02$  ng/mg protein) compared to spared nerve injury–vehicle ( $1.14 \pm 0.05$  ng/mg protein) (fig. 3H; injury  $\times$  treatment,  $F_{1,20} = 5.04$ ;  $P = 0.036$ ; injury,  $F_{1,20} = 2.91$ ;  $P = 0.104$ ; treatment,  $F_{1,20} = 13.44$ ;  $P = 0.002$ ). Spared nerve injury nonstatistically significantly increased DNA/RNA oxidation compared to sham–vehicle ( $0.98 \pm 0.11$  ng/mg protein;  $P = 0.051$ ). There was no effect of dimethyl fumarate in the sham group compared to sham–vehicle.

### Role of NFE2L2 in the Antinociceptive Effects of Dimethyl Fumarate

The next experiments aimed to determine whether activation of the NFE2L2 antioxidant pathway mediated the antinociceptive effects of dimethyl fumarate. First, we administered the NFE2L2 inhibitor trigonelline together with dimethyl fumarate.<sup>37</sup> Trigonelline prevented the reversal of allodynia induced by dimethyl fumarate ( $8.05 \pm 0.21$  g), compared to dimethyl fumarate treatment alone ( $0.46 \pm 0.17$  g) (fig. 4A; time  $\times$  treatment,  $F_{4,40} = 18.33$ ;  $P < 0.001$ ; time,  $F_{2,541,25.41} = 20.53$ ;  $P < 0.001$ ; treatment:  $F_{1,10} = 17.19$ ;  $P = 0.002$ ). Trigonelline did not alter von Frey thresholds in the absence of dimethyl fumarate in the

sham ( $F_{1,397,5.587} = 0.95$ ,  $P = 0.405$ ) or the spared nerve injury conditions (fig. 4A;  $F_{2,583,10.33} = 0.28$ ;  $P = 0.813$ ). Compared to dimethyl fumarate treatment alone, trigonelline cotreatment also reduced the percentage of NFE2L2<sup>+</sup> nuclei in the dorsal root ganglia from rats with spared nerve injury (fig. 4B). Representative photomicrographs are presented in figure 4C.

Next, we administered dimethyl fumarate to wild type and *Nfe2l2*<sup>-/-</sup> male and female mice, beginning 7 days after spared nerve injury when allodynia is fully established in this model.<sup>25</sup> Dimethyl fumarate treatment failed to reverse allodynia in mice lacking *Nfe2l2* ( $0.02 \pm 0.01$  g), while allodynia was alleviated by the treatment in wild type mice ( $0.94 \pm 0.25$  g) (fig. 4D; time  $\times$  treatment,  $F_{4,56} = 38.26$ ;  $P < 0.001$ ; time,  $F_{2,607,36.50} = 37.85$ ;  $P < 0.001$ ; genotype,  $F_{1,14} = 92.70$ ;  $P < 0.001$ ). In this experiment, we also found that allodynia returned several days after the conclusion of dimethyl fumarate treatment in wild type mice (fig. 4D). There were no baseline differences in von Frey threshold between genotypes ( $P = 0.486$ ). As there were no differences between the sexes, data were pooled for analysis.

### Effects on Injured Dorsal Root Ganglia Neurons

Activating transcription factor 3 (ATF3) is a commonly used surrogate marker for neuronal damage after peripheral nerve injury.<sup>38</sup> Strikingly, treatment with dimethyl fumarate reduced the proportion of ATF3<sup>+</sup> nuclei in the spared nerve injury group (10 ATF3<sup>+</sup> nuclei of 102 total nuclei



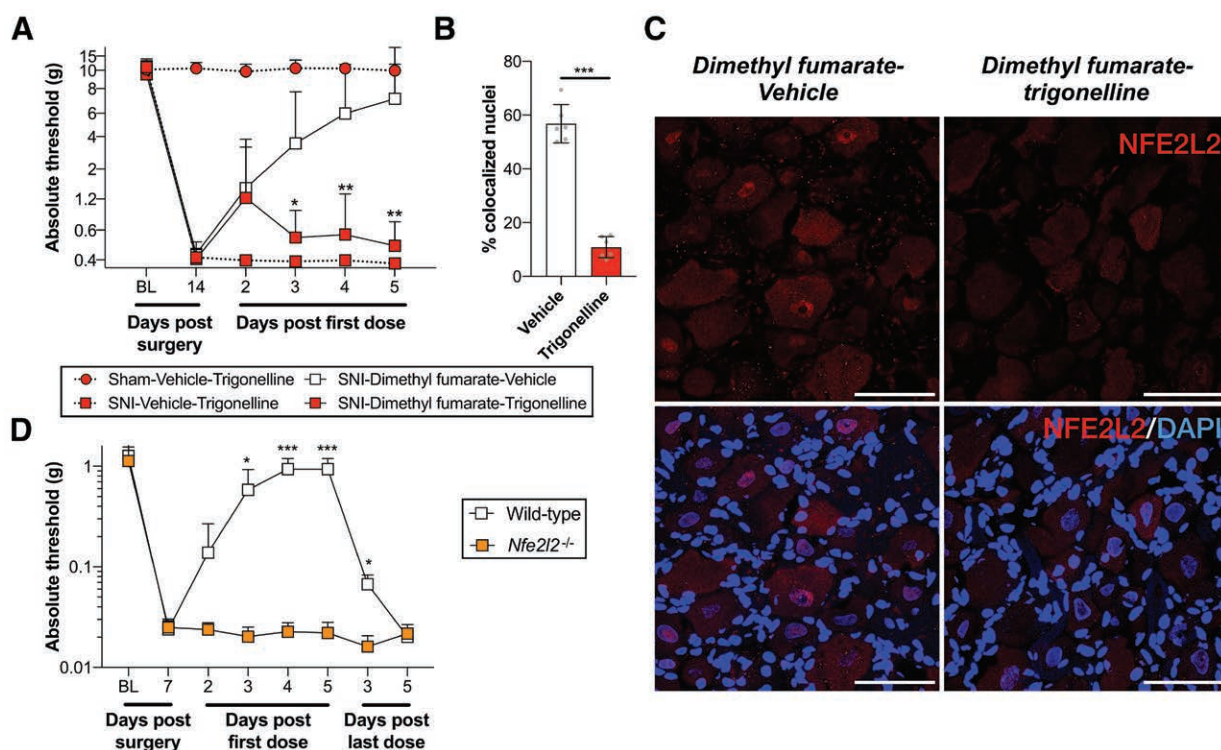


**Fig. 4.** Effects of nuclear factor erythroid 2-related factor 2 (NFE2L2) on antinociceptive effects of dimethyl fumarate. (A) Beginning 14 days after spared nerve injury (SNI) or sham surgery, the NFE2L2 inhibitor trigonelline (300 mg/kg; twice per day) or vehicle was administered together with dimethyl fumarate (300 mg/kg; once per day) or vehicle for 5 days. Von Frey thresholds for mechanical allodynia are presented.  $n = 5$  rats in the sham-vehicle-trigonelline and SNI-vehicle-trigonelline groups;  $n = 6$  rats in all other groups (B, C) Ipsilateral L4/5 dorsal root ganglia (DRG) were collected after 5 days of oral coadministration of the NFE2L2 inhibitor trigonelline (300 mg/kg; twice per day) or vehicle with dimethyl fumarate (300 mg/kg; once per day) or vehicle (Veh), which began 14 days after SNI surgery. NFE2L2 and nuclei were immunofluorescently labeled in DRG sections. (B) The number of 4',6-diamidino-2-phenylindole (DAPI)-positive nuclei colocalized with NFE2L2 are expressed as a percentage of the total number of nuclei in each section. DRG from  $n = 6$  rats/group. (C) Representative fluorescent photomicrographs are presented (40 $\times$ ). Scale bar = 50  $\mu$ m. (D) Beginning 7 days after SNI surgery, dimethyl fumarate (300 mg/kg; once per day) was administered for 5 days to wild type or *Nfe2l2*<sup>-/-</sup> male and female mice ( $n = 4$  per sex). Von Frey thresholds for mechanical allodynia are presented with data pooled from both sexes. Data are mean  $\pm$  SD; \* $P < 0.05$ , \*\* $P < 0.01$ , \*\*\* $P < 0.001$ .

$\pm 1$  of 30) compared to the spared nerve injury-vehicle group (39 of 107  $\pm$  13 of 15) (fig. 5A; injury  $\times$  treatment,  $F_{1,24} = 50.50$ ;  $P < 0.001$ ; injury,  $F_{1,24} = 141.3$ ;  $P < 0.001$ ; treatment,  $F_{1,24} = 53.88$ ;  $P < 0.001$ ). In agreement with a previous study,<sup>39</sup> we found that the percentage of ATF3<sup>+</sup> nuclei in the dorsal root ganglia was increased by  $\sim 38$  fold after spared nerve injury alone, compared to sham-vehicle (1 of 81  $\pm$  1 of 30) and sham-dimethyl fumarate (1 of 118  $\pm$  1 of 24) ( $P < 0.001$ ) (fig. 5A). Representative photomicrographs are presented in figure 5B.

### Impact to Mitochondrial Bioenergetics in Dorsal Root Ganglia Neurons

Redox imbalance disrupts mitochondrial bioenergetics, which is believed to contribute to neuropathic pain.<sup>7,29,40</sup> Therefore, we investigated whether dimethyl fumarate treatment could restore mitochondrial bioenergetics

after spared nerve injury in dorsal root ganglia neurons. Oxygen consumption rates were measured in cultured rat dorsal root ganglia neurons under different conditions (fig. 6A). Dimethyl fumarate treatment completely restored spared nerve injury-induced deficits in basal respiration (fig. 6B; injury  $\times$  treatment,  $F_{1,18} = 5.95$ ;  $P = 0.025$ ; injury,  $F_{1,18} = 11.19$ ;  $P = 0.004$ ; treatment,  $F_{1,18} = 3.78$ ;  $P = 0.068$ ), adenosine triphosphate-linked respiration (fig. 6C; injury  $\times$  treatment,  $F_{1,18} = 3.71$ ;  $P = 0.070$ ; injury,  $F_{1,18} = 14.18$ ;  $P = 0.001$ ; treatment,  $F_{1,18} = 11.58$ ;  $P = 0.003$ ), maximal mitochondrial respiration (fig. 6D; injury  $\times$  treatment:  $F_{1,18} = 7.17$ ;  $P = 0.015$ ; injury,  $F_{1,18} = 4.41$ ;  $P = 0.050$ ; treatment,  $F_{1,18} = 4.41$ ;  $P = 0.017$ ) and spare respiratory capacity (fig. 6E; injury  $\times$  treatment,  $F_{1,18} = 5.28$ ;  $P = 0.034$ ; injury,  $F_{1,18} = 1.90$ ;  $P = 0.185$ ; treatment,  $F_{1,18} = 5.68$ ;  $P = 0.028$ ). Dimethyl fumarate treatment had no effect in the sham group.



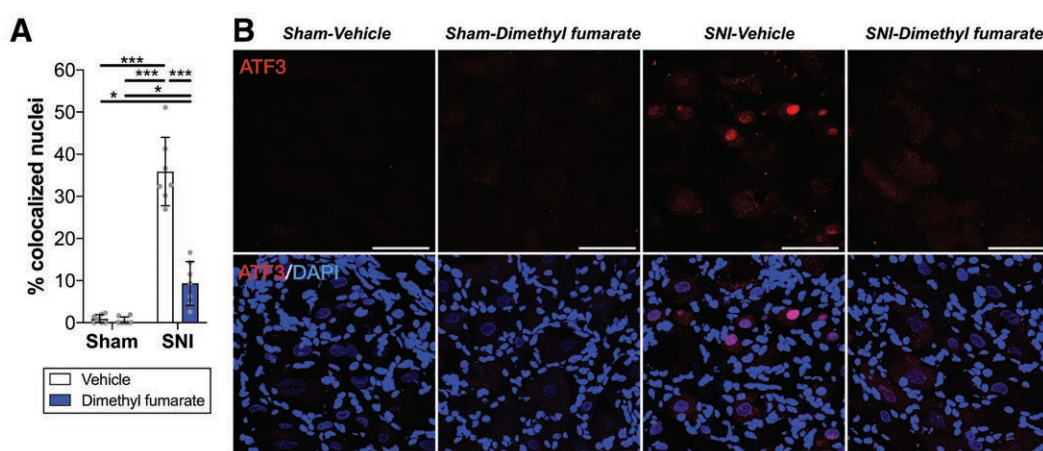


**Fig. 5.** Activating transcription factor 3 (ATF3) levels in lumbar dorsal root ganglia (DRG). Ipsilateral L4/5 DRGs were collected after 5 days of oral dimethyl fumarate treatment (300 mg/kg; once per day) or vehicle, which began 14 days after SNI/sham surgery. ATF3 and 4',6-diamidino-2-phenylindole (DAPI) were immunofluorescently labeled in DRG sections. (A) The number of nuclei colocalized with ATF3 are expressed as a percentage of the total number of nuclei in each section. (B) Representative fluorescent photomicrographs are presented (40 $\times$ ). Data are mean  $\pm$  SD; \* $P$  < 0.05, \*\*\* $P$  < 0.001; DRG from  $n$  = 6 rats/group.

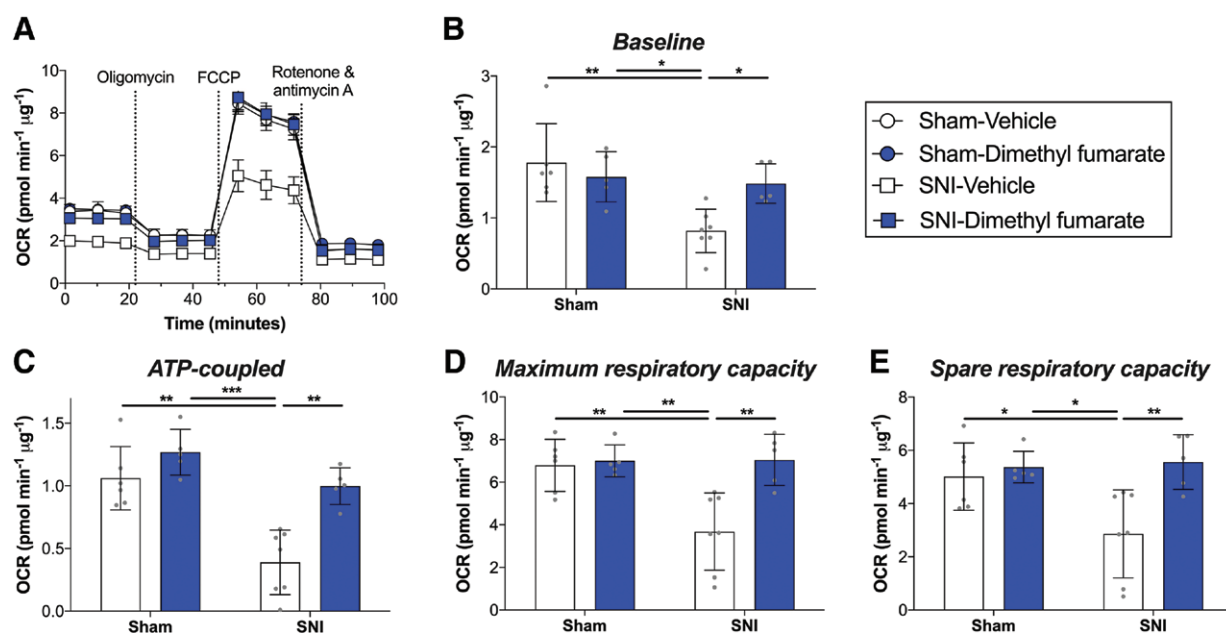


**Fig. 6.** Effects of dimethyl fumarate treatment on mitochondrial bioenergetics after spared nerve injury (SNI). Ipsilateral L4/5 dorsal root ganglia (DRG) were collected and dissociated after 5 days of oral dimethyl fumarate treatment (300 mg/kg; once per day) or vehicle, which began 14 days after SNI/sham surgery. (A) A summary of mitochondrial bioenergetics is presented, and (B) basal respiration, (C) adenosine triphosphate (ATP)-linked respiration (response to oligomycin), (D) maximal mitochondrial respiration (response to carbonyl cyanide-p-trifluoromethoxyphenylhydrazone [FCCP]), and (E) spare respiratory capacity (difference between maximal and basal oxygen consumption rate [OCR]) were quantified. Data are mean  $\pm$  SD; \* $P$  < 0.05, \*\* $P$  < 0.01, \*\*\* $P$  < 0.001; DRG neurons from  $n$  = 5 rats in the sham-dimethyl fumarate and SNI-dimethyl fumarate groups,  $n$  = 6 rats in the sham-vehicle group, and  $n$  = 7 rats in the SNI-vehicle group.

## Effects on Cytokine mRNA Expression and Protein Levels

Proinflammatory cytokines and chemokines are induced downstream of reactive oxygen species, and promote dysfunctional synaptic plasticity that drives neuropathic pain.<sup>7,10</sup> We therefore quantified gene expression and protein levels of the cytokines IL-1 $\beta$  and TNF, and the chemokine CCL2, which have a well-characterized role in neuropathic pain.<sup>7,10</sup> Compared to spared nerve injury–vehicle, treatment with dimethyl fumarate reduced expression of *Il1b* messenger RNA (mRNA) (fig. 7A; injury  $\times$  treatment,  $F_{1,20} = 0.35$ ;  $P = 0.559$ ; injury,  $F_{1,20} = 15.42$ ;  $P < 0.001$ ; treatment,  $F_{1,20} = 17.00$ ;  $P < 0.001$ ) and levels of IL-1 $\beta$  protein (injury–vehicle,  $13.30 \pm 2.95$  pg/mg; injury–dimethyl fumarate,  $6.33 \pm 1.97$  pg/mg) (fig. 7B; injury  $\times$  treatment,  $F_{1,16} = 6.42$ ;  $P = 0.022$ ; injury,  $F_{1,16} = 20.6$ ;  $P < 0.001$ ; treatment,  $F_{1,16} = 27.8$ ;  $P < 0.001$ ). *Il1b* mRNA and IL-1 $\beta$  protein were increased after spared nerve injury, compared to sham (fig. 7, A to C). Spared nerve injury–induced increases in *Ccl2* mRNA (fig. 7C; injury  $\times$  treatment,  $F_{1,20} = 6.75$ ;  $P = 0.017$ ; injury,  $F_{1,20} = 32.34$ ;  $P < 0.001$ ; treatment,  $F_{1,20} = 16.03$ ;  $P < 0.001$ ) and CCL2 protein levels (injury–vehicle,  $4.28 \pm 0.30$  ng/mg; injury–dimethyl fumarate,  $2.30 \pm 0.47$  ng/mg) (fig. 7D; injury  $\times$  treatment,  $F_{1,16} = 43.41$ ;  $P < 0.001$ ; injury,  $F_{1,16} = 140.5$ ;  $P < 0.001$ ; treatment,  $F_{1,16} = 54.67$ ;  $P < 0.001$ ) were also alleviated by dimethyl fumarate treatment. *Tnf* mRNA expression was reduced by dimethyl fumarate (fig. 7E; injury  $\times$  treatment,  $F_{1,20} = 1.25$ ;  $P = 0.28$ ; injury,  $F_{1,20} = 5.70$ ;  $P = 0.027$ ; treatment,  $F_{1,20} = 20.53$ ;  $P < 0.001$ ), but TNF protein was not detected in any sample.

## Discussion

We discovered that dimethyl fumarate is an effective treatment for neuropathic pain behaviors and mechanisms in rats and mice. This effect is mediated by activation of NFE2L2 that can increase expression of antioxidants. Reactive oxygen species and their by-products are a key molecular node for neuropathic pain; they promote excitability in pain pathways by directly activating nociceptive neurons, impairing mitochondrial bioenergetics, and inducing transcription of proinflammatory cytokines.<sup>7,8,10,11</sup> Spared nerve injury did not consistently induce redox imbalance among the markers that we quantified, which may be a function of assay sensitivity and the single timepoint that was assessed. Nonetheless, we demonstrated that dimethyl fumarate alleviated pain mechanisms that are driven by oxidative stress, including injury to dorsal root ganglia neurons (ATF3<sup>+</sup>), disrupted mitochondrial bioenergetics, and increased levels of proinflammatory and pronociceptive cytokines.

The beneficial effects of dimethyl fumarate are mediated through activation of NFE2L2, as we showed that the antiallodynic effects were lost when the NFE2L2 inhibitor trigonelline was coadministered, or when dimethyl

fumarate was administered to *Nfe2l2*<sup>-/-</sup> mice. The activation (nuclear translocation) of NFE2L2 by dimethyl fumarate was confirmed immunohistochemically and by quantifying protein in nuclear extracts. While the morphology suggests that NFE2L2 is activated in neurons, future studies could characterize the cell populations in which NFE2L2 is activated after dimethyl fumarate treatment. In addition, dimethyl fumarate increased the expression and activity of antioxidants that are targets of NFE2L2, and decreased oxidized RNA/DNA. These data provide converging evidence that activation of NFE2L2, rather than other possible mechanisms,<sup>42–44</sup> is the major therapeutic target of dimethyl fumarate for spared nerve injury.

Dimethyl fumarate treatment attenuated levels of ATF3 and restored mitochondrial bioenergetics in dorsal root ganglia neurons. There is precedent for these effects, as dimethyl fumarate was found to promote neuroregeneration after sciatic nerve crush injury,<sup>41</sup> and was cytoprotective in experimental autoimmune encephalomyelitis models.<sup>23</sup> Future studies could therefore test whether dimethyl fumarate attenuates Wallerian degeneration in the spared nerve injury model. Restored mitochondrial bioenergetics, as found here, may also explain the reduction in injured neurons, as mitochondrial dysfunction is noted to cause degeneration of primary afferents;<sup>40</sup> restored mitochondrial function may therefore be upstream of reduced ATF3 levels. That treatment was able to reverse existing functional deficits of mitochondria, and possibly neuronal damage, highlights the disease-modifying potential of dimethyl fumarate. However, these antinociceptive mechanisms may not persist, as allodynia returned when dimethyl fumarate was discontinued in mice.

Dimethyl fumarate activated NFE2L2 in the sham-operated animals, but it did not cause a concomitant increase in expression or activity of antioxidants. These data suggest that despite nuclear translocation of NFE2L2, the antioxidant response element may not be activated due to negative regulation. Nerve injury may be required for adequate levels of small musculoaponeurotic fibrosarcoma (sMaf) proteins that dimerize with NFE2L2 and facilitate DNA binding.<sup>12</sup> The expression of sMaf gene transcripts is increased by proinflammatory cytokines<sup>45</sup> that are elevated by nerve injury.<sup>10,11</sup> This could lead to lower sMaf levels in the sham condition that reduce the ability for NFE2L2 to dimerize and activate the antioxidant response element. BTB domain and CNC homolog 1 (Bach1), a transcriptional repressor of the promoter region to which NFE2L2 binds,<sup>12,13</sup> could serve as another regulatory factor. It is possible that Bach1 displacement is facilitated after peripheral nerve injury to allow NFE2L2 binding, which would also account for our results. These hypotheses, however, require testing.

Relatedly, our data also reveal that NFE2L2 is only modestly activated in response to spared nerve injury in the absence of drug treatment. Why this endogenous resolution mechanism is not engaged in response to the oxidative stress that

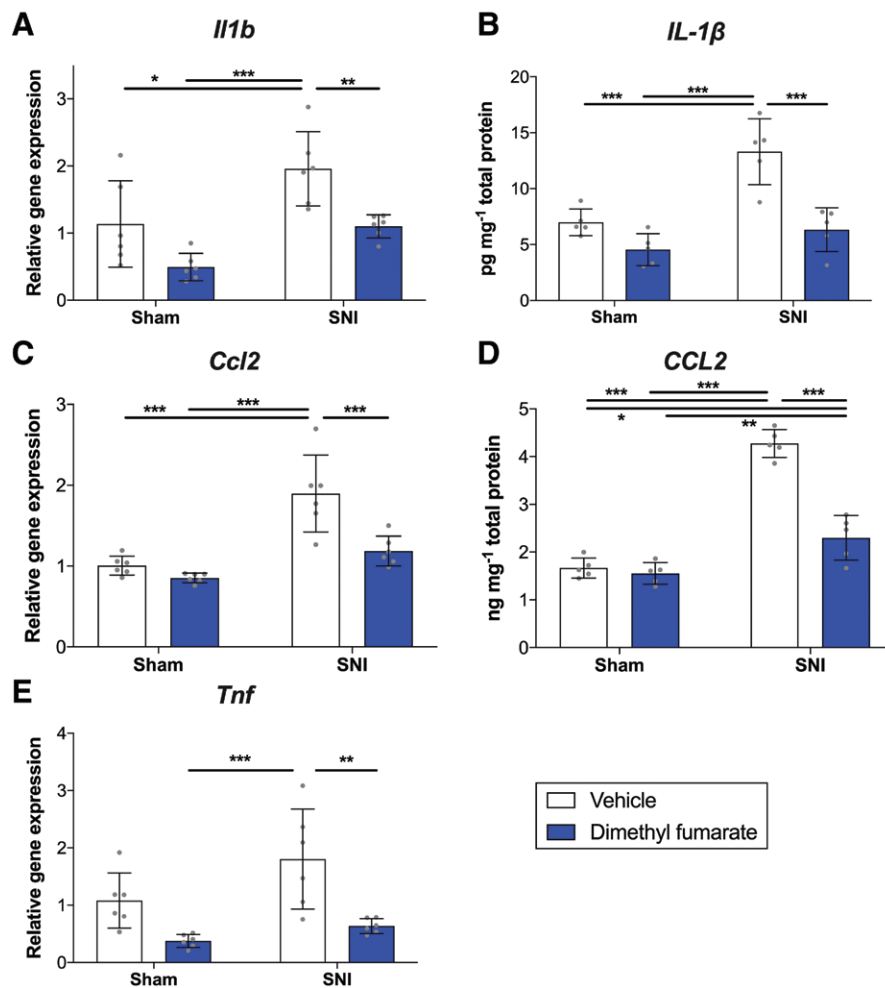


**Fig. 7.** Effects of dimethyl fumarate treatment on expression of proinflammatory cytokines. Ipsilateral L4/5 dorsal root ganglia (DRG) were collected after 5 days of oral dimethyl fumarate treatment (300 mg/kg; once per day) or vehicle, which began 14 days after spared nerve injury (SNI)/sham surgery. Messenger RNA (mRNA) expression was quantified for (A) *Il1b*, (C) *Ccl2*, and (E) *Tnf*; protein levels for (B) *IL-1β* and (D) *CCL2* were assayed. Data are mean  $\pm$  SD; \* $P$  < 0.05, \*\* $P$  < 0.01, \*\*\* $P$  < 0.001; DRG from  $n$  = 6 rats/group.

occurs after peripheral nerve injury remains an open question. One explanation could be that total levels of NFE2L2 are reduced in the pain neuraxis after peripheral nerve injury, as reported by other groups.<sup>18,46</sup> However, the mechanisms that may underlie downregulation of NFE2L2 require elucidation.

In this study, we restricted our mechanistic investigations to the dorsal root ganglia. However, monomethyl fumarate, the active metabolite of dimethyl fumarate, is central nervous system-penetrant and likely affects nociceptive signaling in the spinal cord, brainstem, and cortex. In support, direct infusion of monomethyl fumarate into the central nucleus of the amygdala alleviated vocalizations and neuronal hyperactivity in a mouse model of arthritis.<sup>47</sup> Future mechanistic studies will therefore be directed toward spinal and supraspinal sites, after systemic administration of dimethyl fumarate.

Dimethyl fumarate successfully reversed allodynia in wild type mice of both sexes. We also found that dimethyl fumarate efficacy was abolished in *Nfe2l2*-deficient male and female mice. These data suggest that the therapeutic effects of dimethyl fumarate in the spared nerve injury model are gated through NFE2L2 in a sex-independent manner. However, a limitation of our study and potential source of bias was that the mechanistic experiments used only male rats as an economic consideration. A number of studies have now identified sex differences in mechanisms that underlie nociceptive hypersensitivity after nerve injury, particularly with respect to neuroimmune mechanisms.<sup>48–50</sup> Thus, the NFE2L2-dependent antinociceptive effects of dimethyl fumarate could be driven by different mechanisms in each sex. These questions will be addressed in future studies.



It should be noted that dimethyl fumarate may not be well tolerated in some patients. Common adverse effects include flushing, abdominal pain, nausea, and diarrhea, while leukopenia can occur under rarer circumstances.<sup>20</sup> In a Letter to the Editor, moderate-to-severe articular and musculoskeletal pain was reported in three patients after dimethyl fumarate treatment for relapsing–remitting multiple sclerosis,<sup>51</sup> which runs counter to the results presented in this study. However, the frequency of painful adverse effects induced by dimethyl fumarate is unknown and needs to be quantitatively surveyed. Furthermore, it is not clear if painful effects only occur in patients with inflammatory disorders. Future studies could improve the tolerability of dimethyl fumarate by refining fumaric acid esters to develop new therapeutics with disease-modifying potential for peripheral neuropathic pain-related behaviors and underlying mechanisms.

In summary, we illustrate the ability for oral dimethyl fumarate to resolve behavioral signs of peripheral neuropathic pain *via* activation of NFE2L2, with concomitant attenuation of several underlying pronociceptive mechanisms. An advantage of dimethyl fumarate is that it is already approved for multiple sclerosis by the U.S. Food and Drug Administration and European Medicines Agency; clinical investigations could commence to determine whether dimethyl fumarate can be repurposed for disease-modifying treatment of neuropathic pain.

### Research Support

Supported by U.S. Army Medical Research and Materiel Command grant No. W81XWH-16-1-0717 (Fort Detrick, Frederick, Maryland), MD Anderson Cancer Center (Houston, Texas) Startup funds, a University of Texas System (Austin, Texas) Rising STARs award (to Dr. Grace) and National Institutes of Health grant Nos. R01 NS073939, R01 CA227064 (Bethesda, Maryland; to Dr. Kavelaars). Development of the mechanical conflict-avoidance procedure was supported by a subcontract from Manzanita Pharmaceuticals (Woodside, California) to Dr. Walters.

### Competing Interests

Dr. Grace is a named inventor on a patent application covering the use of fumaric acid esters for treatment of neuropathic pain.

### Correspondence

Address correspondence to Dr. Grace: 6565 MD Anderson Blvd, Houston, Texas 77030. PGrace@mdanderson.org. Information on purchasing reprints may be found at [www.anesthesiology.org](http://www.anesthesiology.org) or on the masthead page at the beginning of this issue. ANESTHESIOLOGY's articles are made freely accessible to all readers, for personal use only, 6 months from the cover date of the issue.

### References

1. Hecke O van, Austin SK, Khan RA, Smith BH, Torrance N: Neuropathic pain in the general population: A systematic review of epidemiological studies. *Pain* 2014; 155:654–62
2. Gaskin DJ, Richard P: The economic costs of pain in the United States. *J Pain* 2012; 13:715–24
3. Finnerup NB, Attal N, Haroutounian S, McNicol E, Baron R, Dworkin RH, Gilron I, Haanpää M, Hansson P, Jensen TS, Kamerman PR, Lund K, Moore A, Raja SN, Rice AS, Rowbotham M, Sena E, Siddall P, Smith BH, Wallace M: Pharmacotherapy for neuropathic pain in adults: A systematic review and meta-analysis. *Lancet Neurol* 2015; 14:162–73
4. Volkow ND, McLellan AT: Opioid abuse in chronic pain—Misconceptions and mitigation strategies. *N Engl J Med* 2016; 374:1253–63
5. Borsook D, Hargreaves R, Bountra C, Porreca F: Lost but making progress—Where will new analgesic drugs come from? *Sci Transl Med* 2014; 6:249sr3
6. Price TJ, Basbaum AI, Bresnahan J, Chambers JF, Koninck YD, Edwards RR, Ji R-R, Katz J, Kavelaars A, Levine JD, Porter L, Schechter N, Sluka KA, Terman GW, Wager TD, Yaksh TL, Dworkin RH: Transition to chronic pain: Opportunities for novel therapeutics. *Nature Reviews Neuroscience* 2018; 19:383–4
7. Grace PM, Gaudet AD, Staikopoulos V, Maier SF, Hutchinson MR, Salvemini D, Watkins LR: Nitroxidative signaling mechanisms in pathological pain. *Trends Neurosci* 2016; 39:862–79
8. Salvemini D, Little JW, Doyle T, Neumann WL: Roles of reactive oxygen and nitrogen species in pain. *Free Radic Biol Med* 2011; 51:951–66
9. Kallenborn-Gerhardt W, Schröder K, Geisslinger G, Schmidtke A: NOXious signaling in pain processing. *Pharmacol Ther* 2013; 137:309–17
10. Grace PM, Hutchinson MR, Maier SF, Watkins LR: Pathological pain and the neuroimmune interface. *Nat Rev Immunol* 2014; 14:217–31
11. Ji RR, Chamessian A, Zhang YQ: Pain regulation by non-neuronal cells and inflammation. *Science* 2016; 354:572–7
12. Satoh T, Lipton S: Recent advances in understanding NRF2 as a druggable target: Development of pro-electrophilic and non-covalent NRF2 activators to overcome systemic side effects of electrophilic drugs like dimethyl fumarate. *F1000Res* 2017; 6:2138
13. Cuadrado A, Rojo AI, Wells G, Hayes JD, Cousin SP, Rumsey WL, Attucks OC, Franklin S, Levonen AL, Kensler TW, Dinkova-Kostova AT: Therapeutic targeting of the NRF2 and KEAP1 partnership in chronic diseases. *Nat Rev Drug Discov* 2019; 18:295–317
14. Negi G, Kumar A, Sharma SS: Nrf2 and NF-κB modulation by sulforaphane counteracts multiple

- manifestations of diabetic neuropathy in rats and high glucose-induced changes. *Curr Neurovasc Res* 2011; 8:294–304
15. Kim D, You B, Jo EK, Han SK, Simon MI, Lee SJ: NADPH oxidase 2-derived reactive oxygen species in spinal cord microglia contribute to peripheral nerve injury-induced neuropathic pain. *Proc Natl Acad Sci U S A* 2010; 107:14851–6
  16. Rosa AO, Egea J, Lorrio S, Rojo AI, Cuadrado A, López MG: Nrf2-mediated haeme oxygenase-1 up-regulation induced by cobalt protoporphyrin has antinociceptive effects against inflammatory pain in the formalin test in mice. *Pain* 2008; 137:332–9
  17. Yang Y, Luo L, Cai X, Fang Y, Wang J, Chen G, Yang J, Zhou Q, Sun X, Cheng X, Yan H, Lu W, Hu C, Cao P: Nrf2 inhibits oxaliplatin-induced peripheral neuropathy via protection of mitochondrial function. *Free Radic Biol Med* 2018; 120:13–24
  18. Ferreira-Chamorro P, Redondo A, Riego G, Leánez S, Pol O: Sulforaphane inhibited the nociceptive responses, anxiety- and depressive-like behaviors associated with neuropathic pain and improved the anti-allodynic effects of morphine in mice. *Front Pharmacol* 2018; 9:1332
  19. Li S, Yang C, Fang X, Zhan G, Huang N, Gao J, Xu H, Hashimoto K, Luo A: Role of Keap1-Nrf2 signaling in anhedonia symptoms in a rat model of chronic neuropathic pain: Improvement with sulforaphane. *Front Pharmacol* 2018; 9:887
  20. Xu Z, Zhang F, Sun F, Gu K, Dong S, He D: Dimethyl fumarate for multiple sclerosis. *Cochrane Database Syst Rev* 2015:CD011076 doi:10.1002/14651858.CD011076.pub2
  21. Gold R, Kappos L, Arnold DL, Bar-Or A, Giovannoni G, Selma J, Tornatore C, Sweetser MT, Yang M, Sheikh SI, Dawson KT; DEFINE Study Investigators: Placebo-controlled phase 3 study of oral BG-12 for relapsing multiple sclerosis. *N Engl J Med* 2012; 367:1098–107
  22. Ahuja M, Ammal Kaidery N, Yang L, Calingasan N, Smirnova N, Gaisin A, Gaisina IN, Gazaryan I, Hushpalian DM, Kaddour-Djebbar I, Bollag WB, Morgan JC, Ratan RR, Starkov AA, Beal MF, Thomas B: Distinct Nrf2 signaling mechanisms of fumaric acid esters and their role in neuroprotection against 1-methyl-4-phenyl-1,2,3,6-tetrahydropyridine-induced experimental Parkinson's-like disease. *J Neurosci* 2016; 36:6332–51
  23. Linker RA, Lee DH, Ryan S, van Dam AM, Conrad R, Bista P, Zeng W, Hronowsky X, Buko A, Chollate S, Ellrichmann G, Brück W, Dawson K, Goelz S, Wiese S, Scannevin RH, Lukashev M, Gold R: Fumaric acid esters exert neuroprotective effects in neuroinflammation via activation of the Nrf2 antioxidant pathway. *Brain* 2011; 134(Pt 3):678–92
  24. Decosterd I, Woolf CJ: Spared nerve injury: An animal model of persistent peripheral neuropathic pain. *Pain* 2000; 87:149–58
  25. Shields SD, Eckert WA 3<sup>rd</sup>, Basbaum AI: Spared nerve injury model of neuropathic pain in the mouse: A behavioral and anatomic analysis. *J Pain* 2003; 4:465–70
  26. Chaplan SR, Bach FW, Pogrel JW, Chung JM, Yaksh TL: Quantitative assessment of tactile allodynia in the rat paw. *J Neurosci Methods* 1994; 53:55–63
  27. Grace PM, Fabisiak TJ, Green-Fulgham SM, Anderson ND, Strand KA, Kwilas AJ, Galer EL, Walker FR, Greenwood BN, Maier SF, Fleshner M, Watkins LR: Prior voluntary wheel running attenuates neuropathic pain. *Pain* 2016; 157:2012–23
  28. Grace PM, Strand KA, Galer EL, Urban DJ, Wang X, Baratta MV, Fabisiak TJ, Anderson ND, Cheng K, Greene LI, Berkelhammer D, Zhang Y, Ellis AL, Yin HH, Campeau S, Rice KC, Roth BL, Maier SF, Watkins LR: Morphine paradoxically prolongs neuropathic pain in rats by amplifying spinal NLRP3 inflammasome activation. *Proc Natl Acad Sci U S A* 2016; 113:E3441–50
  29. Krukowski K, Ma J, Golonzhka O, Laumet GO, Gutti T, van Duzer JH, Mazitschek R, Jarpe MB, Heijnen CJ, Kavelaars A: HDAC6 inhibition effectively reverses chemotherapy-induced peripheral neuropathy. *Pain* 2017; 158:1126–37
  30. Treutwein B, Strasburger H: Fitting the psychometric function. *Percept Psychophys* 1999; 61:87–106
  31. Harvey LO: Efficient estimation of sensory thresholds. *Behavior Research Methods, Instruments, & Computers* 1986; 18:623–32
  32. Harte SE, Meyers JB, Donahue RR, Taylor BK, Morrow TJ: Mechanical conflict system: A novel operant method for the assessment of nociceptive behavior. *PLoS One* 2016; 11:e0150164
  33. Odem MA, Lacagnina MJ, Katzen SL, Li J, Wicks KC, Spence EA, Grace PM, Walters ET: Persistent postsurgical pain caused by sham surgeries for three neuropathic pain models is indicated by behavioral alterations in an operant conflict test. *PAIN* 2019; 160:2440–55
  34. Grace PM, Shimizu K, Strand KA, Rice KC, Deng G, Watkins LR, Herson PS: (+)-Naltrexone is neuroprotective and promotes alternative activation in the mouse hippocampus after cardiac arrest/cardiopulmonary resuscitation. *Brain Behav Immun* 2015; 48:115–22
  35. Grace PM, Strand KA, Galer EL, Rice KC, Maier SF, Watkins LR: Protraction of neuropathic pain by morphine is mediated by spinal damage associated molecular patterns (DAMPs) in male rats. *Brain Behav Immun* 2018; 72:45–50
  36. Maj MA, Ma J, Krukowski KN, Kavelaars A, Heijnen CJ: Inhibition of mitochondrial p53 accumulation by

- PFT- $\mu$  prevents cisplatin-induced peripheral neuropathy. *Front Mol Neurosci* 2017; 10:108
37. Boettler U, Sommerfeld K, Volz N, Pahlke G, Teller N, Somoza V, Lang R, Hofmann T, Marko D: Coffee constituents as modulators of Nrf2 nuclear translocation and ARE (EpRE)-dependent gene expression. *J Nutr Biochem* 2011; 22:426–40
  38. Tsujino H, Kondo E, Fukuoka T, Dai Y, Tokunaga A, Miki K, Yonenobu K, Ochi T, Noguchi K: Activating transcription factor 3 (ATF3) induction by axotomy in sensory and motoneurons: A novel neuronal marker of nerve injury. *Mol Cell Neurosci* 2000; 15:170–82
  39. Laedermann CJ, Pertin M, Suter MR, Decosterd I: Voltage-gated sodium channel expression in mouse DRG after SNI leads to re-evaluation of projections of injured fibers. *Mol Pain* 2014; 10:19
  40. Bennett GJ, Doyle T, Salvemini D: Mitotoxicity in distal symmetrical sensory peripheral neuropathies. *Nat Rev Neurol* 2014; 10:326–36
  41. Szezanowski F, Donaldson DM, Hartung HP, Mausberg AK, Kleinschnitz C, Kieseier BC, Stettner M: Dimethyl fumarate accelerates peripheral nerve regeneration via activation of the anti-inflammatory and cytoprotective Nrf2/HO-1 signaling pathway. *Acta Neuropathol* 2017; 133:489–91
  42. Schulze-Topphoff U, Varrin-Doyer M, Pekarek K, Spencer CM, Shetty A, Sagan SA, Cree BA, Sobel RA, Wipke BT, Steinman L, Scannevin RH, Zamvil SS: Dimethyl fumarate treatment induces adaptive and innate immune modulation independent of Nrf2. *Proc Natl Acad Sci U S A* 2016; 113:4777–82
  43. Kornberg MD, Bhargava P, Kim PM, Putluri V, Snowman AM, Putluri N, Calabresi PA, Snyder SH: Dimethyl fumarate targets GAPDH and aerobic glycolysis to modulate immunity. *Science* 2018; 360:449–53
  44. Boccella S, Guida F, De Logu F, De Gregorio D, Mazzitelli M, Belardo C, Ianotta M, Serra N, Nassini R, de Novellis V, Geppetti P, Maione S, Luongo L: Ketones and pain: Unexplored role of hydroxyl carboxylic acid receptor type 2 in the pathophysiology of neuropathic pain. *FASEB J* 2019; 33:1062–73
  45. Massrieh W, Derjuga A, Doualla-Bell F, Ku CY, Sanborn BM, Blank V: Regulation of the MAFF transcription factor by proinflammatory cytokines in myometrial cells. *Biol Reprod* 2006; 74:699–705
  46. Arruri V, Komirishetty P, Areti A, Dungavath SKN, Kumar A: Nrf2 and NF- $\kappa$ B modulation by Plumbagin attenuates functional, behavioural and biochemical deficits in rat model of neuropathic pain. *Pharmacol Rep* 2017; 69:625–32
  47. Kim H, Thompson J, Ji G, Ganapathy V, Neugebauer V: Monomethyl fumarate inhibits pain behaviors and amygdala activity in a rat arthritis model. *Pain* 2017; 158:2376–85
  48. Lopes DM, Malek N, Edye M, Jager SB, McMurray S, McMahon SB, Denk F: Sex differences in peripheral not central immune responses to pain-inducing injury. *Sci Rep* 2017; 7:16460
  49. Sorge RE, Mapplebeck JC, Rosen S, Beggs S, Taves S, Alexander JK, Martin LJ, Austin JS, Sotocinal SG, Chen D, Yang M, Shi XQ, Huang H, Pillion NJ, Bilan PJ, Tu Y, Klip A, Ji RR, Zhang J, Salter MW, Mogil JS: Different immune cells mediate mechanical pain hypersensitivity in male and female mice. *Nat Neurosci* 2015; 18:1081–3
  50. North RY, Li Y, Ray P, Rhines LD, Tatsui CE, Rao G, Johansson CA, Zhang H, Kim YH, Zhang B, Dussor G, Kim TH, Price TJ, Dougherty PM: Electrophysiological and transcriptomic correlates of neuropathic pain in human dorsal root ganglion neurons. *Brain* 2019; 142:1215–26
  51. Bernardini LR, Zecca C, Clerici VT, Gobbi C, Mantegazza R, Rossi S: Severe articular and musculoskeletal pain: An unexpected side effect of dimethyl-fumarate therapy for multiple sclerosis. *J Neurol Sci* 2016; 369:139–40